

Plio-Quaternary landscape evolution in the uplifted Ardennes: New insights from $^{26}\text{Al}/^{10}\text{Be}$ data from cave-deposited alluvium (Meuse catchment, E Belgium)

Gilles Rixhon^{a,b,*}, Régis Braucher^c, Didier L. Bourlès^c, Alexandre Peeters^d, Alain Demoulin^{d,e}, Laetitia Léanni^c, Georges Aumaître^c, Karim Keddadouche^c

^a Laboratoire Image, Ville, Environnement (LIVE UMR 7362), Université de Strasbourg, 3 rue de l'Argonne, 67000 Strasbourg, France

^b Ecole Nationale du Génie de l'Eau et de l'Environnement de Strasbourg (ENGEE), 1 quai Koch, 67000 Strasbourg, France

^c Centre Européen de Recherche et d'Enseignement de Géosciences de l'Environnement (CEREGE), Technopôle de l'Arbois-Méditerranée, BP80, 13545 Aix-en-Provence, France

^d Department of Geography, University of Liège, Clos Mercator 3, Liège 4000, Belgium

^e F.R.S.-FNRS, Rue d'Egmont, 5, Brussels 1000, Belgium

ARTICLE INFO

Article history:

Received 18 April 2019

Received in revised form 7 September 2020

Accepted 7 September 2020

Available online xxx

Keywords

Landscape evolution

Cave-deposited alluvium

$^{26}\text{Al}/^{10}\text{Be}$ burial dating

River incision

ABSTRACT

Despite a wealth of recent studies dealing with the evolution of the drainage network in the uplifted Ardennes massif (E. Belgium), especially from the Middle Pleistocene onwards, the Ardennian landscape evolution and long-term incision rates in the Meuse catchment remain poorly documented over the whole Plio-Quaternary. Alluvium-filled multilevel cave systems represent a relevant setting to unravel the Late Cenozoic history of regional river incision. We present here a dataset of $^{26}\text{Al}/^{10}\text{Be}$ concentration data obtained from fifteen pebble samples washed into the Chawresse system, one of the largest multi-level cave systems of Belgium, which developed in Devonian limestones of the lower Ourthe valley, the main Ardennian tributary of the Meuse. The sample collection spans an elevation difference higher than 120 m and their depleted $^{26}\text{Al}/^{10}\text{Be}$ ratios yield burial ages ranging from ~0.25 to 3.28 Ma. After critical assessment of our dataset for intra-karstic reworking issues, the most striking outcome of the obtained burial ages is the acceleration by a factor five of the incision rates (from ~30 to ~150 m/Ma) during the first half of the Middle Pleistocene. Integrating this incision peak and our pre-burial denudation rates, we then revisit the existing framework of Plio-Quaternary denudation and river incision in the Ardennian Meuse catchment. Whilst our $^{26}\text{Al}/^{10}\text{Be}$ concentration data shed new light on the temporal and spatial variability of the local river and hillslope system response to coupled tectonic and climatic forcings, it simultaneously highlights sampling issues and the need for further chronological data.

© 2020

1. Introduction

Beyond studies embracing the western part of the Rhenish shield (e.g., Meyer et al., 1983; Demoulin and Hallot, 2009), the Neogene and Quaternary landscape evolution of the Variscan Ardennes massif, i.e., its westernmost area, has long been a core topic of western Europe geomorphology. In this framework, the Ardennian Meuse catchment has received particular attention (Davis, 1895). The first geomorphic works focused on either Cenozoic erosion surfaces (e.g., Alexandre, 1976; Demoulin, 1995) or Quaternary river terrace systems of the Meuse (e.g., Macar, 1975; Juvigné and Renard, 1992; Pisart et al., 1997) and its Ardennian tributaries (e.g. Ek, 1957; Juvigné, 1979; Cornet, 1995). However, most of them did not go much

beyond the mere reconstruction of successive landform generations. During the last twenty years, studies based on DEM analysis, modern dating methods, and numerical modelling have provided new insights into the quantitative long-term evolution of the Ardennian Meuse catchment. They allowed, for instance, the determination of sediment budgets (Van Balen et al., 2000) and palaeodenudation rates (Schaller et al., 2002, 2004; Demoulin et al., 2009), dating of river terrace deposits (Rixhon et al., 2011, 2014), modelling of knickpoint propagation (Beckers et al., 2014) and hillslope denudation (Bovy et al., 2016).

Despite these significant advances, the timing of Ardennian landscape evolution over the Plio-Quaternary remains poorly documented (Rixhon and Demoulin, 2018). In this respect, although the Ardennes massif is well-known for hosting spectacular cave systems developed in Paleozoic limestone formations at the outskirts of its siliceous core, such as the Han-sur-Lesse cave (e.g., Quinif and Hallet, 2018), little effort has been made so far to use this favourable setting to unravel long-term landscape evolution. Importantly, multi-level cave

* Corresponding author at: Laboratoire Image, Ville, Environnement (LIVE UMR 7362), Université de Strasbourg, 3 rue de l'Argonne, 67000 Strasbourg, France.

E-mail address: gilles.rixhon@live-cnrs.unistra.fr (G. Rixhon)

systems may record massif-scale fluvial history. Penetrating into the karstic system as bedload of sinking streams, sediments may be left behind as flowing water abandons the cave when diversion of the underground stream to a lower topographic level occurs (Anthony and Granger, 2007). As they point to the last period of time during which the passage was at the local water table, fluvial sediments deposited in higher-lying abandoned phreatic passages, mimicking alluvium-mantled terrace sequences (Granger et al., 1997), are useful archives to unravel the timing of river incision. In this respect, in situ-produced cosmogenic nuclides are a powerful tool to quantify the pace of long-term river incision (e.g., Rixhon et al., 2017), either through depth-profile dating of alluvial terraces (e.g., Repka et al., 1997) or burial dating of fluvial sediments washed into caves (e.g., Granger et al., 1997). Here, we apply this last approach.

This study explores whether past episodes of fluvial base-level stability in the Ardennes can be chronologically constrained via $^{26}\text{Al}/^{10}\text{Be}$ burial dating of ancient, alluvium-filled karstic passages in one of the largest multi-level cave systems of Belgium. Coarse fluvial sediments were sampled for ^{10}Be and ^{26}Al measurements in the so-called Chawresse system located in the lower Ourthe Valley (i.e., the largest Ardennian tributary of the Meuse), whose karstic levels span an elevation range >120 m. We thereby primarily aim to constrain long-term incision rates at the northern rim of the uplifted Ardennes massif. Complementing the existing ~ 0.4 Ma age of the younger main terrace in the lower Ourthe Valley (Rixhon et al., 2011), new $^{26}\text{Al}/^{10}\text{Be}$ burial ages ranging from ~ 0.2 to 3.3 Ma extend the reconstructed incision history to the Plio-Quaternary. In addition, $^{26}\text{Al}/^{10}\text{Be}$ ratios provide pre-burial denudation rate estimates.

2. Geologic and geomorphic setting of the study area

2.1. Late Cenozoic uplift of the Rhenish-Ardennes massif

The Ardennes constitutes the western part of the Paleozoic Rhenish massif in southeastern Belgium (Fig. 1a). The whole Ardennes-Rhenish massif experienced Late Cenozoic tectonic uplift, claimed to have been caused by either lithospheric thinning (e.g., Prodehl et al., 1995), lithospheric folding (e.g., Cloetingh et al., 2005), or mantle upwelling beneath S. Eifel (Ritter et al., 2001). Whereas the spatial pattern of mid-Pleistocene uplift has been usually interpreted as an epeirogenic dome centered on the Eifel (Meyer and Stets, 1998; Van Balen et al., 2000), Demoulin and Hallot (2009) recently suggested that an uplift pulse migrated northwards across the massif, pointing to lithospheric folding as the primary cause of uplift.

About 400–450 m of rock uplift has been inferred for the Rhenish massif since the Oligocene (Demoulin and Hallot, 2009). Up to 150 m deep Quaternary river incision in the Ardennes bears witness to a recently increased uplift pace probably occurring in two steps, first at the Pliocene-Pleistocene transition and then sometime at the beginning of the Middle Pleistocene (Van Balen et al., 2000). During this last, short-lasting uplift pulse (probably a few 10^4 yr), rock uplift peak rates may have reached 0.3 to 0.5 mm/yr (Fig. 1a; Van Balen et al., 2000; Demoulin and Hallot, 2009; Rixhon and Demoulin, 2018). A phase of tectonic quiescence is postulated from the late Middle Pleistocene onwards (Van Balen et al., 2000).

2.2. The Ourthe catchment and its lower valley reach

The Ourthe, largest Ardennian tributary of the Meuse, joins it at the northern rim of the massif in Liège at an elevation of ~ 60 m (Figs. 1b and 2). Its ~ 3600 km² catchment is characterized by a highly asymmetric drainage network, the main stem closely following its western border. From south to north, the Ourthe Valley is incised into the siliceous Lower Devonian basement of the Ardennes anticlinorium and rock strata of the Dinant Synclinorium, including limestone formations

of the Middle/Upper Devonian and Carboniferous at several locations (Fig. 1b). Owing to sustained karstification processes, many large cave systems developed directly along the Ourthe Valley in both Devonian (Bohon, Hotton, Chawresse caves; e.g., Bastin et al., 1988) and Carboniferous limestone formations (Abîme, Nou Bleu caves; e.g., Peeters and Ek, 2018).

The ~ 30 km long lower reach of the Ourthe Valley records a Late Cenozoic incision amounting to a maximum of >130 m (Cornet, 1995). Previous geomorphic works reconstructed up to 20 terrace levels along this reach (Ek, 1957; Cornet, 1995) (Fig. 2). However, these reconstructions are essentially descriptive and lack reliable chronological data to constrain the timing of river downcutting. The lowest terrace at Tilff is dated by the presence of the Early Glacial Rocourt tephra (0.074–0.090 Ma), close to the study area (Juvigné, 1973; Pouclet et al., 2008), thereby suggesting a mean incision rate in the order of 40 m/Ma since the onset of the last glaciation. The only other numerical age, obtained by Rixhon et al. (2011) via a ^{10}Be depth profile, is 0.39 ± 0.04 Ma for the abandonment time of the Younger Main Terrace (YMT) of the Ourthe at Colonster (~ 3 km downstream of the Chawresse area). The YMT is a fundamental marker in the Ardennian valleys because it is located at the hinge between the broad Early Pleistocene upper part of the valleys' transverse profile and their nested deeply incised Middle Pleistocene lower part (Rixhon and Demoulin, 2018). The YMT tread is perched ~ 55 m above the modern floodplain (all relative elevations provided hereafter refer to the level of the Ourthe modern floodplain at the Chawresse confluence), yielding a mean incision rate of 141 ± 15 m/Ma in this reach since 0.39 Ma.

As for mean denudation rates in the Ardennes, Schaller et al. (2004) calculated rates increasing from 30 m/Ma before 0.7 Ma to 60–80 m/Ma after that time, based on the ^{10}Be content of terrace sediments whose age is estimated using a MIS correlation. These rate estimates, however, refer to the timespan of hillslope erosion preceding sediment deposition in the valley bottom. By contrast, Demoulin et al. (2009) inferred a lower average rate of 27 m/Ma since ~ 0.7 Ma over the entire Ourthe catchment, based on geomorphic estimates of river incision and interfluvial denudation.

2.3. The Chawresse multi-level cave system

Located ~ 12 km upstream of the Ourthe-Meuse confluence at Liège (Figs. 1b and 2), the partly subaerial, partly subterranean Chawresse stream is a small tributary deeply incised into the eastern valley side of the lower Ourthe. Its tiny catchment (~ 3 km²) comprises Lower/Middle Devonian siliceous rocks in the headwaters area and Upper Devonian limestone in its downstream part (Fig. 3a). It hosts one of the largest and best-documented multi-level cave systems of Belgium in strongly folded and faulted Frasnian limestone (e.g. Ek, 1961; Ek and Poty, 1982; De Bie, 2013) (Fig. 3b–c). We will call it hereafter the Chawresse cave system. It stretches in the WSW-ENE Chawresse Valley to more than 1.5 km from the confluence, includes more than 10 km of karstic galleries and shafts, and spans a total elevation difference exceeding 135 m (De Bie, 2013; Fig. 4). Along with secondary, smaller caves, the interconnected Chawresse system encompasses five main cave developments named Victor, Chawresse, Veronika, Manants and Sainte-Anne, from the highest to the lowest. According to De Bie (2013), the total length and vertical height difference of each of these caves amount to ~ 180 and ~ 47 m (Victor), ~ 5650 and ~ 81 m (Chawresse and Veronika taken as a single development, see below), ~ 1650 and ~ 67 m (Manants) and ~ 1750 and ~ 35 m (Sainte-Anne). Their interconnection is attested either by narrow passages such as between Chawresse and Veronika (leading De Bie, 2013 to propose a single development stage for these two caves) or by fluorescent dye

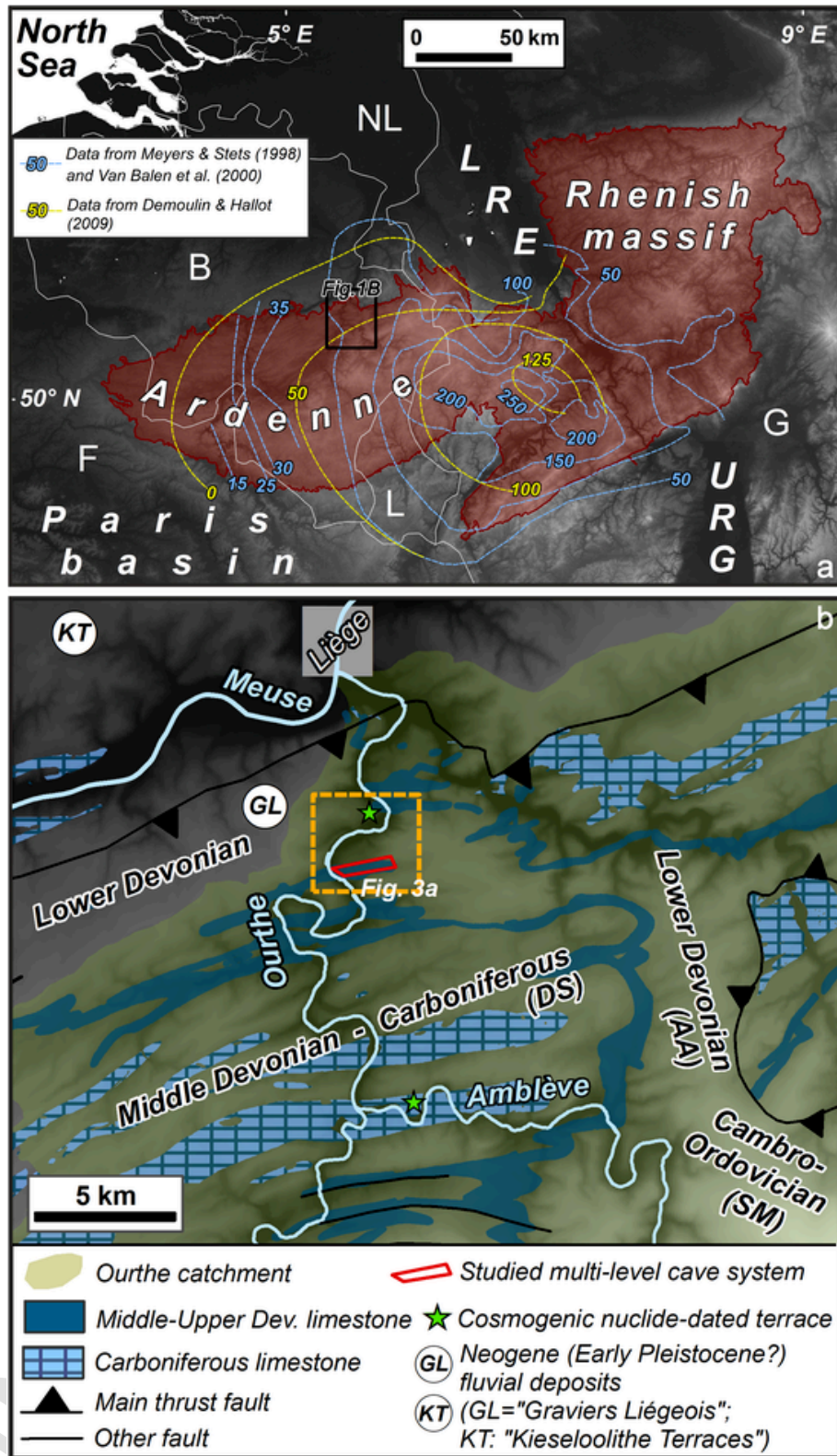


Fig. 1. a. Location of the Paleozoic Ardennes/Rhenish massif in northern Europe (reddish area), with blue and yellow dashed lines referring to the estimated amount of uplift (m) since the beginning of the Middle Pleistocene (Demoulin and Hallot, 2009 explicitly referring to the tectonic component of uplift). LRE: Lower Rhine embayment; URG: Upper Rhine graben. b. Simplified geological map of the northern Ourthe catchment, highlighting the two main karstified limestone formations. The investigated Chawresse multi-level cave system is located with the red frame. Remnants of the oldest alluvial deposits in this area ("Graviers Liégeois-GL") and the oldest terraces deposits of the Meuse ("Kieseloolithe Terraces-KT") are located by white circles. AA, DS, and SM refer to Ardennes Anticlinorium, Dinant Synclinorium and Stavelot Massif, respectively. The dashed orange rectangle refers to Fig. 3a. (For interpretation of the references to color in this figure legend, the reader is referred to the web version of this article.)

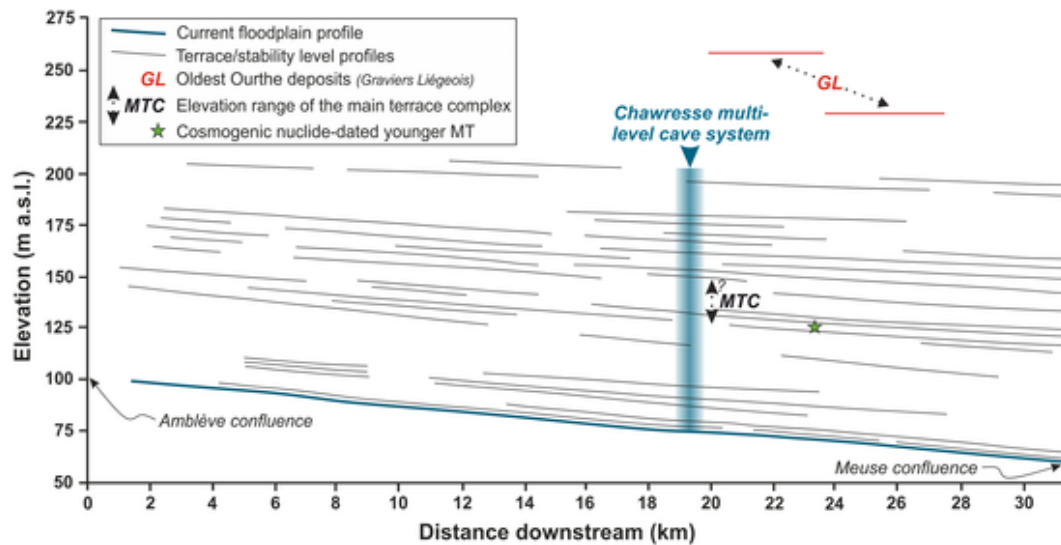


Fig. 2. Lower Ourthe Valley: longitudinal profile of the modern floodplain and previous stability levels (up to 20 different according to Cornet, 1995), chiefly inferred from terrace remnants and karstic phreatic tubes, such as those from the Chawresse multi-level system (see Fig. 4). The profile reconstruction is modified from Cornet (1995).

tracing such as between Victor and Sainte-Anne (Fig. 4; Supplementary material 1).

Speleogenetic studies in the Chawresse system agree to highlight the presence of well-developed, abandoned subhorizontal phreatic tubes at different elevations, usually exhibiting an elliptical cross section, as the main morphological feature (Ek, 1961, 1964; Ek and Poty, 1982; De Bie, 2013) (Fig. 5a). These tubes constitute most of Sainte-Anne (at ~12 and 20 m relative elevation, see e.g., Ek, 1964) and Veronika, with extensions into the Chawresse cave (at ~70 and 75–78 m relative elevation, see De Bie, 2013). The polycyclic nature of these phreatic levels has long been recognized in Sainte-Anne (Ek, 1961) and may be assumed for the whole system, matching a *per descensum* model of karstification (Harmand et al., 2017). In the frame of a tectonically controlled gradual base-level lowering, authors agree that there is a morphogenic correlation between cave development and the subaerial terrace sequence in the lower Ourthe Valley (Ek, 1961; Quinif, 1989; Cornet, 1995). (See Fig. 6.)

The main abandoned phreatic tubes in the Chawresse and Veronika caves are roughly located at the same relative elevations, but vadose shafts and canyons, almost absent in Veronika, build an intricate network in the Chawresse cave (Fig. 4). Although similarity of elevation favours the hypothesis of a single stage of cave development, the contrast in shaft and canyon density argues against it, though this contrast might be controlled by the local geological structure. Indeed, whereas the main phreatic passages of Veronika stretch along the anticlinal hinge, all developments of the Chawresse cave are located within the steeply dipping southern limb of the anticline, ~50 m more to the south. The Manants cave, which seems to have developed geographically apart from the other cave systems, is dominated by abundant vadose shafts and canyons. The bulk of these occur in the southern wall of the Chawresse Valley, spanning >65 m of elevation difference similar to those of the Chawresse cave (Fig. 4). The current entrance of the Manants cave corresponds to an active sinkhole in the sub-aerial Chawresse streambed (Figs. 3a and 4b). At the base of the cave development, poorly developed phreatic tubes are aligned along the ENE continuation of the main phreatic developments of the Sainte-Anne cave (Fig. 4). Caver explorations report an intricate underground topography for the Manants karstic system (De Bie, 2013). A peculiarity of Sainte-Anne is that the ceiling of one of the phreatic tubes displays a >1 m high dissolution feature, which might have been caused by sediment accumulating in this formerly water-filled passage and

inducing upward dissolution of the tube's ceiling (i.e., paragensis, Farant, 2004; see Fig. 5b). This indicates that the alluvium that once filled this passage could have been almost completely evacuated by the underground Chawresse stream as a response to a later drop of the water table.

3. Sampling strategy and $^{26}\text{Al}/^{10}\text{Be}$ burial dating

A two-step scenario constitutes the basic prerequisite of burial dating applied to cave-deposited alluvium, namely exposure at the (sub-)surface followed by a rapid and complete burial at a depth great enough (practically, >20 m of overburden) to efficiently prevent any postburial muonic production (e.g., Granger, 2014). It also assumes that, once the clastic sediments had entered the underground karstic system, they suffered no erosion or underground reworking (e.g., Rixhon, 2016). Therefore, wherever possible (i) we primarily targeted cave passages where clastic infills were massively preserved (as in the Veronika cave, see Supplementary material 1), (ii) we preferentially sampled underground sediments that still exhibit original tiling and bedding structures in the abandoned phreatic tubes (Fig. 5c–d) and (iii) we avoided deposits for which reworking could obviously be suspected (for instance, those located close to active passages of the underground Chawresse stream). Given the generally coarse size of the cave sediments, the pebble fraction was selected (Supplementary material 1). Altogether, fifteen quartz-bearing samples, chiefly quartz pebbles with subsidiary quartzite pebbles, were collected (Fig. 5d; Supplementary material 2). Twelve out of the fifteen processed samples were single clast samples, the three others, all extracted from the Manants cave (MAN1, 2 and 3bis), were amalgamated samples (Table 1, Supplementary material 2). Whilst two samples were taken in the Victor cave at relative elevations of ~125 and 135 m, we purposely collected more samples in the main phreatic developments of the lower-lying cave levels in order to strengthen the timing of the main phases of fluvial base-level stability in the lower Ourthe Valley (Fig. 4 and Table 1). We thus collected four or five samples from the Veronika cave (relative elevation of ~72 to 75 m), the Manants cave (~15 to 35 m) and Sainte-Anne cave (~12 to 20 m). Note that $^{26}\text{Al}/^{10}\text{Be}$ burial dating of cave-deposited alluvium constrains the last period of time during which the passage was at the local water table. In the case of prior ghost-rock karstification (Dubois et al., 2014), this is also the time when ghost-rock feature emptying could be achieved, allowing for sediments originating from the ground surface to be brought into the passage.

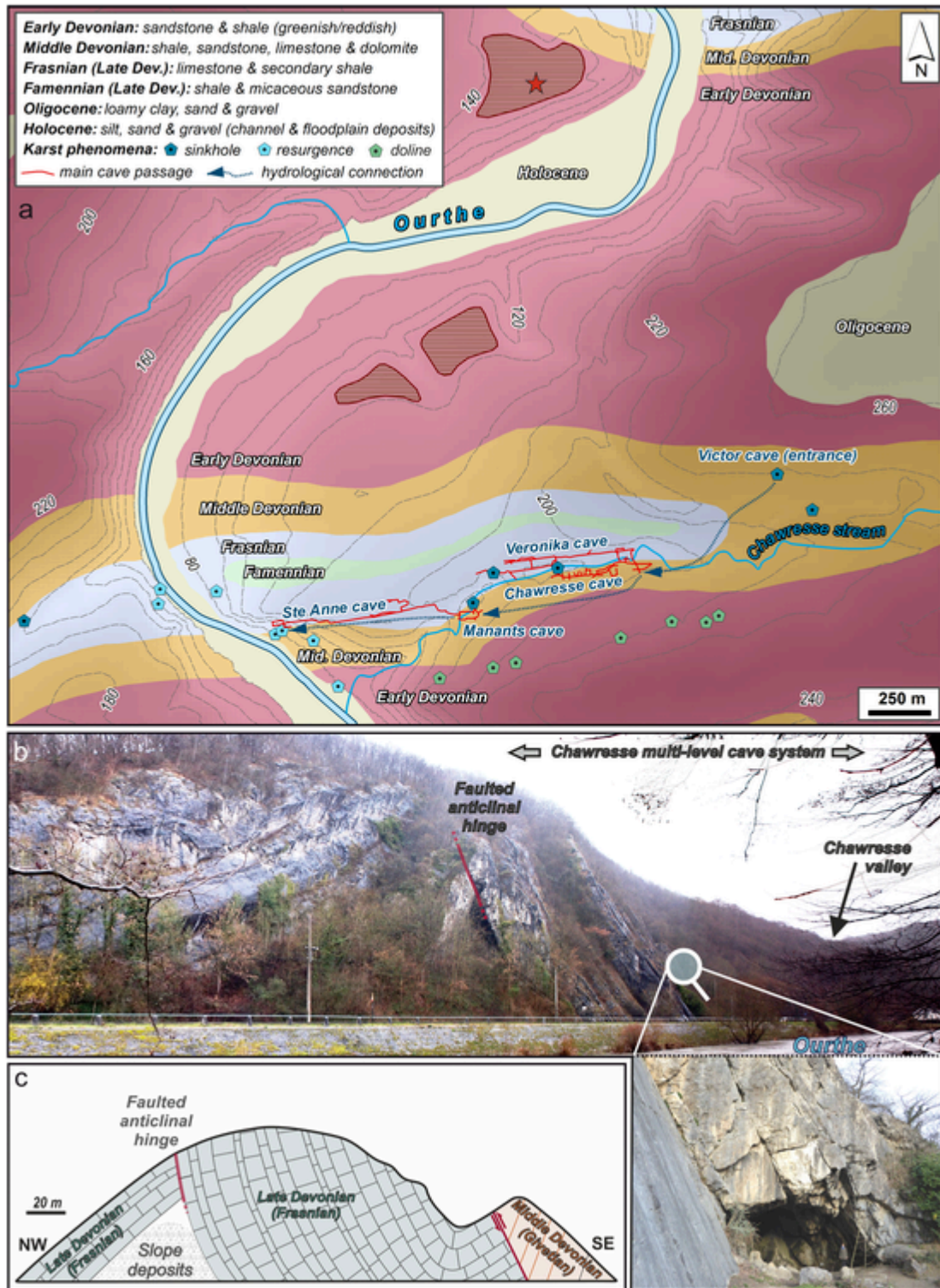


Fig. 3. a. Geological map of the study area and the Chawresse multi-level cave system. Red dashed areas and red star refer to remnants of the younger main terrace and the sampling location for depth profile dating in the Colonster terrace (Rixhon et al., 2011), respectively. Lithology and karst phenomena are extracted from De Bie (2013) and the hydrogeological map of Wallonia (Ruthy, 2015). b. Panoramic view of the folded Frasnian limestone from the western Ourthe Valley wall (photo: G. Rixhon). The entrenched Chawresse Valley is visible to the south. The spectacular Sainte-Anne cave's entrance is perched ~17 m above the current river channel (see the person for scale; photo: G. Rixhon). c. Simplified geological sketch of the eastern valley side alongside the main road (adapted from Ek, 2007). (For interpretation of the references to color in this figure legend, the reader is referred to the web version of this article.)

The burial duration is estimated from measurements of the $^{26}\text{Al}/^{10}\text{Be}$ ratio, which decreases with burial time according to the different disintegration rates of the two radionuclides (e.g., Dunai, 2010;

Rixhon, 2016; see Supplementary material 3 for mathematical development). In this study, we used half-lives of $(1.387 \pm 0.012) \times 10^6$ and $(0.705 \pm 0.017) \times 10^6$ yr for ^{10}Be and ^{26}Al , respectively (Granger, 2006; Chmeleff et al., 2010; Korschinek et al., 2010).

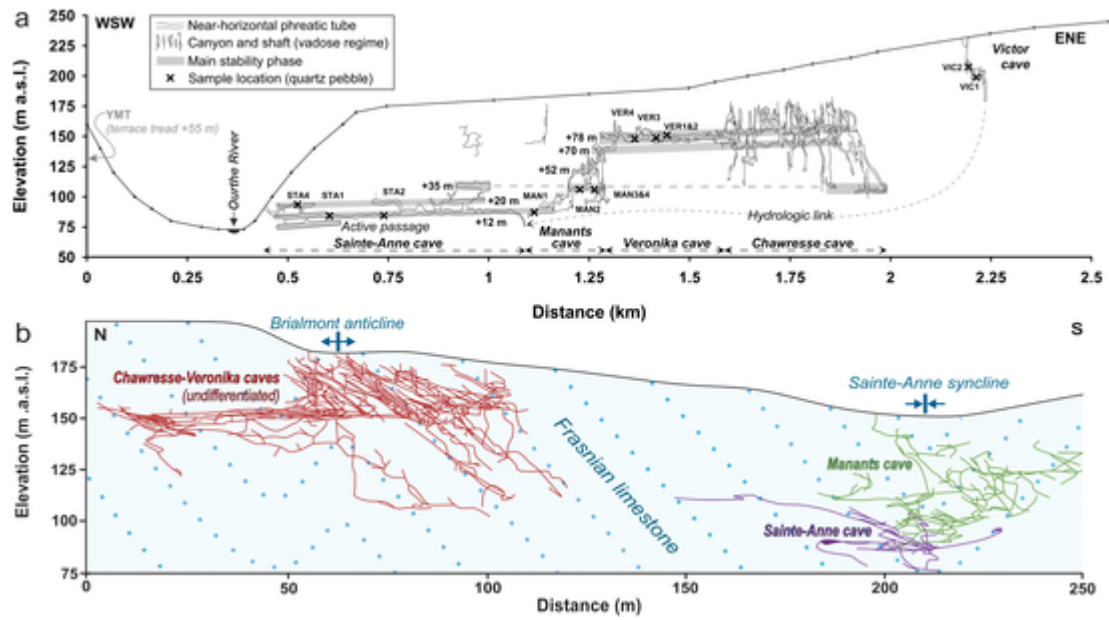


Fig. 4. Cross sections of the lower Ourthe Valley with the projected cave levels of the Chawresse multi-level system. a. WSW-ENE-oriented, topographic cross section exhibiting the location of the fifteen samples (quartz and quartzite pebbles) collected from the oldest cave system (Victor) to the youngest (Sainte-Anne). The underground topography is adapted from Ek (1961) for the Sainte-Anne cave and De Bie (2013) for all other cave levels. The elevation of the Younger Main Terrace (YMT) is also reported. b. Simplified, N-S-oriented, geological cross section (quasi-perpendicular to that of Fig. 4a). Note the relationship between local structure and cave development: the Chawresse/Veronika caves and the Manants/Sainte-Anne caves are mostly developed in relationship with an anticlinal and synclinal structure, respectively. Adapted from De Bie (2013).



Fig. 5. Field photos from the multi-level Chawresse cave system a. Elliptical cross section of the active phreatic tube with a twofold notch in the main level of Sainte-Anne (photo: V. Gerber). b. Probable paragenetic feature in the ceiling of a phreatic tube of Sainte-Anne (dashed red curve; photo: V. Gerber); c. Tiling structure of the elongated pebbles (dashed white arrows) indicating the palaeo-flow direction of the underground stream in the main phreatic level of Veronika (from Rixhon, 2016). d. Alternation of matrix-supported (M-S) and clast-supported (C-S) layers in river sediments filling the main phreatic tube of Veronika, and sampling location of the quartz pebble VER1 (photo: Y. Levecq). (For interpretation of the references to color in this figure legend, the reader is referred to the web version of this article.)

The chemical treatment and the AMS measurements (both ^{10}Be and ^{26}Al) of all samples presented in this study were carried out at the CEREGE laboratory in Aix-en-Provence. After crushing and sieving (be-

tween 1 and 0.250 mm), sediment samples passed through magnetic separation, and the non-magnetic fraction underwent selective etching in fluorosilicic and hydrochloric acids to eliminate all mineral phases

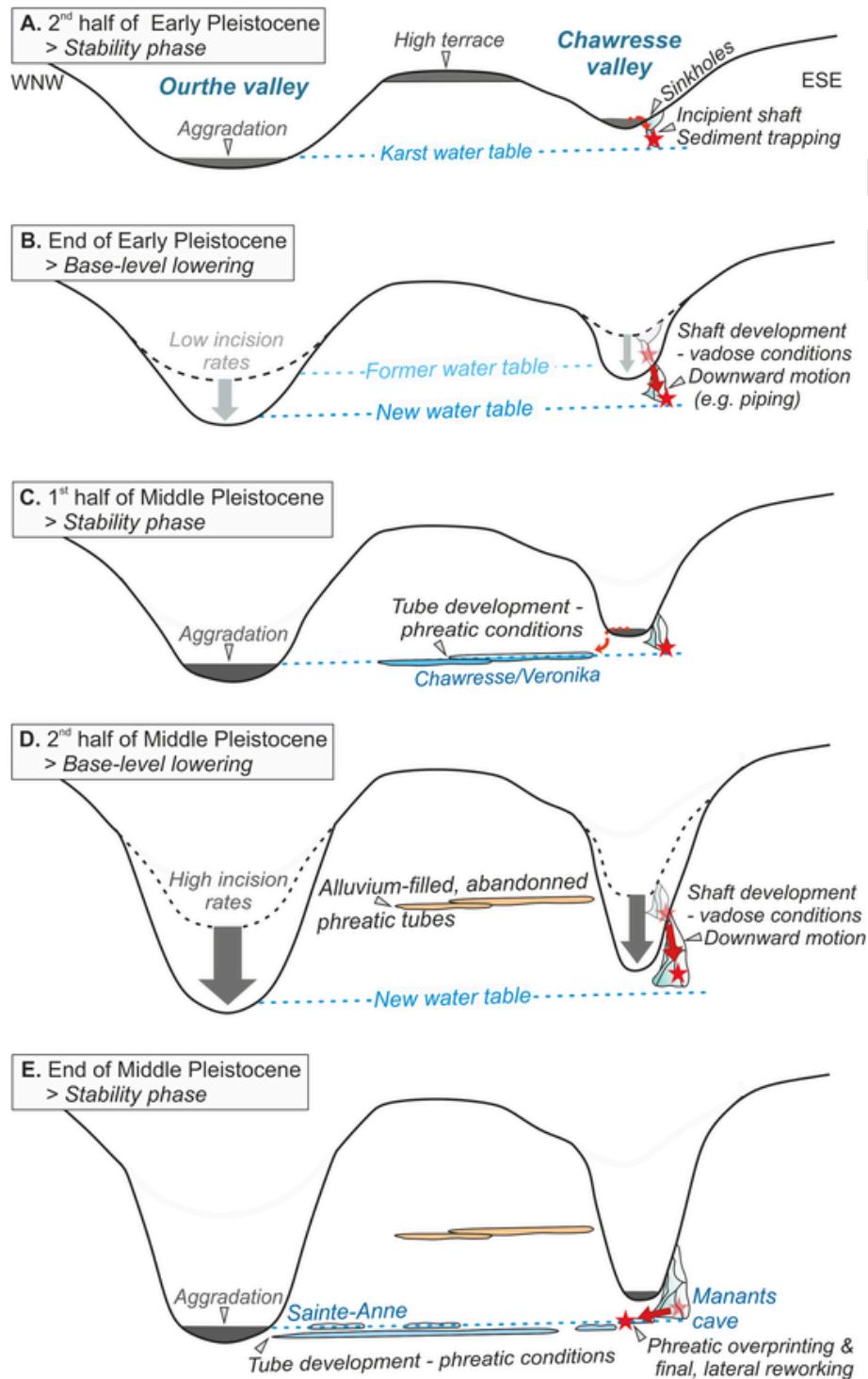


Fig. 6. Long-term, *per descensum*, speleogenetic scenario involving gradual base-level lowering and proposing an uncoupled evolution of the Chawresse/Veronika caves and Manants/Sainte-Anne caves. It shows a stepwise intra-karsting reworking of the clasts sampled in the Manants cave (red stars), which yielded “abnormally” old burial ages (see text for further explanation). Grey arrows refer to river incision whereas thin dotted and thick red arrows represent sediment motion at the surface and in the underground karstic system, respectively. (For interpretation of the references to color in this figure legend, the reader is referred to the web version of this article.)

but quartz. Quartz minerals then underwent a series of selective etchings in hydrofluoric acid to eliminate potential surface contamination by ^{10}Be produced in the atmosphere (Brown et al., 1991). The cleaned quartz minerals were then completely dissolved in hydrofluoric acid after addition in each sample of $\sim 100\ \mu\text{l}$ of an in-house carrier solution ($(3.025 \pm 0.009) \times 10^{-3}\ \text{g}\ ^9\text{Be/g}$ solution) prepared from a deep-mined phenakite (Merchel et al., 2008). After substituting HF

by HNO_3 , an aliquot of $500\ \mu\text{l}$ of the obtained solution was taken for ^{27}Al concentration measurements. Aluminum and beryllium were separated from the remaining solution by ion-exchange chromatography and selective precipitation (Merchel and Herpers, 1999). The resulting Be and Al precipitates were oxidized by heating at $800\ ^\circ\text{C}$ for 1 h and the oxides were mixed to 325 mesh niobium powder prior to measurements by Accelerator Mass Spectrometry (AMS). All the data re-

Table 1

Results of the ^{10}Be and ^{26}Al concentration measurements with the $^{26}\text{Al}/^{10}\text{Be}$ ratios, from which the burial ages (Ma) and palaeodenudation rates (i.e., before the burial event in m/Ma) are computed. Based on an average elevation of 240 m for the Chawresse catchment, the Stone scaling factor amounts to 1.2845. No postburial production was considered. All uncertainties are 1-sigma.

Caves + sampling elevation/sample ID + nature ^a	$^{10}\text{Be}/^9\text{Be}$	Uncert.	^{10}Be	Uncert.	$^{26}\text{Al}/^{27}\text{Al}$	Uncert.	^{26}Al	Uncert.	$^{26}\text{Al}/^{10}\text{Be}$	Unc.	Burial age	Unc.	Palaeoden. rate	Uncert.
			(atoms/g)	(atoms/g)			(atoms/g)	(atoms/g)			(Ma)	(Ma)	(m/Ma)	(m/Ma)
Victor (~125–135 m of relative elevation)														
VIC1 (sing.cl.)	4.54E-13	1.42E-14	384,317	12,047	4.86E-13	4.56E-14	459,703	43,170	1.20	0.12	3.28	0.22	1.44	0.24
VIC2 (sing.cl.)	1.23E-13	4.01E-15	112,284	3664	6.46E-13	5.35E-14	642,531	53,452	5.72	0.51	0.38	0.24	29.28	4.16
Veronika (~72–75 m of relative elevation)														
VER1 (sing.cl.)	3.72E-13	1.27E-14	334,415	11,478	3.57E-13	1.88E-14	1,709,349	95,295	5.11	0.33	0.56	0.18	8.08	1.01
VER2 (sing.cl.)	7.21E-13	2.28E-14	601,930	19,161	6.62E-13	2.78E-14	3,464,437	158,767	5.76	0.32	0.26	0.15	4.97	0.55
VER3 (sing.cl.)	1.85E-12	4.30E-14	2,356,386	55,297	6.76E-12	2.06E-13	9,886,421	310,034	4.20	0.16	0.50	0.08	0.81	0.07
VER4 (sing.cl.)	1.68E-13	5.48E-15	146,529	4809	1.88E-13	1.41E-14	791,373	60,736	5.40	0.45	0.51	0.23	20.26	2.89
Manants (~15–35 m of relative elevation)														
MAN1 (amalg.)	1.57E-13	5.00E-15	150,426	4825	5.61E-13	6.76E-14	595,834	72,042	3.96	0.50	1.13	0.32	14.15	2.65
MAN2 (amalg.)	3.99E-13	1.25E-14	352,449	11,115	6.12E-13	3.64E-14	1,020,973	61,616	2.90	0.20	1.66	0.17	4.14	0.51
MAN3 (sing.cl.)	3.66E-13	1.25E-14	312,034	10,703	6.80E-13	4.17E-14	853,539	52,711	2.74	0.19	1.79	0.18	4.42	0.58
MAN3bis (amalg.)	2.04E-13	6.50E-15	180,981	5776	6.33E-13	4.88E-14	619,189	47,933	3.42	0.29	1.41	0.22	9.94	1.41
Sainte-Anne (~12–18 m of relative elevation)														
STA1 (sing.cl.)	2.50E-13	8.08E-15	217,928	7075	1.50E-13	1.17E-14	1,024,054	79,680	4.70	0.40	0.77	0.22	11.54	1.65
STA1bis (sing.cl.)	8.44E-13	2.88E-14	737,993	25,269	1.62E-12	6.26E-14	2,988,746	116,123	4.05	0.21	0.89	0.13	2.77	0.30
STA2 (sing.cl.)	6.27E-14	3.17E-15	62,250	3151	3.45E-13	4.62E-14	381,841	51,205	6.13	0.88	0.24	0.38	58.27	11.92
STA2bis (sing.cl.)	3.40E-13	1.16E-14	332,018	11,374	1.30E-12	6.39E-14	1,933,862	95,615	5.82	0.35	0.30	0.16	9.47	1.11
STA4 (sing.cl.)	1.51E-13	7.23E-15	132,752	6383	7.67E-14	9.21E-15	571,828	68,700	4.31	0.56	0.94	0.36	18.32	3.94

^a Sample nature: single-clast sample (*sing.cl.*); amalgamated sample (*amalg.*); see also Supplementary material 2.

ported in this study have been measured at the French national facility ASTER of the CEREGE. Beryllium-10 data were calibrated directly versus the National Institute of Standards and Technology standard reference material NIST SRM 4325 using an assigned $^{10}\text{Be}/^{9}\text{Be}$ value of $(2.79 \pm 0.03) \times 10^{-11}$ (Nishiizumi et al., 2007). This standardization is equivalent to 07KNSTD within rounding error. The obtained $^{26}\text{Al}/^{27}\text{Al}$ ratios were calibrated against the ASTER in-house standard SM-Al-11 with $^{26}\text{Al}/^{27}\text{Al} = 7.401 \pm 0.064 \times 10^{-12}$, which has been cross-calibrated against the primary standards certified by a laboratory inter-calibration exercise (Merchel and Bremser, 2004). ^{27}Al concentrations, naturally present in the samples, were measured at CEREGE by ICP-OES. Analytical uncertainties (reported as 1σ) include uncertainties associated with AMS counting statistics, AMS internal error (0.5%), chemical blank measurement and, regarding ^{26}Al , ^{27}Al measurement. Long-term measurements of chemically processed blanks yield ratios on the order of $3.0 \pm 1.5 \times 10^{-15}$ for ^{10}Be and $2.2 \pm 2.0 \times 10^{-15}$ for ^{26}Al (Arnold et al., 2010).

A local ^{10}Be production rate of $5.16 \text{ g at}^{-1} \text{ yr}^{-1}$ was obtained using local coordinates, an average catchment elevation of 240 m and a sea-level high latitude production rate of $P_0 = (4.02 \pm 0.36) \text{ at g}^{-1} \text{ yr}^{-1}$ (Stone, 2000). The latter is identical to the weighted mean of production rates in the Northern Hemisphere (Ruszkiczay-Rüdiger et al., 2016) and in agreement with recently calibrated values (Borchers et al., 2016). An $^{26}\text{Al}/^{10}\text{Be}$ pre-burial, spallation production ratio amounting to 6.61 was used (Nishiizumi et al., 1989; Braucher et al., 2011). Because the cave overburden is always thicker than 20 m, post-burial muon production was ignored in the burial age determination.

4. Results: $^{26}\text{Al}/^{10}\text{Be}$ ratios, burial ages and pre-burial denudation rates

Cosmogenic ^{10}Be and ^{26}Al concentrations in the samples range between $(0.62 \pm 0.03) \times 10^5$ and $(23.56 \pm 0.55) \times 10^5$, and $(3.82 \pm 0.51) \times 10^5$ and $(98.86 \pm 3.10) \times 10^5$ atoms g^{-1} quartz, respectively (Table 1). These concentrations yield $^{26}\text{Al}/^{10}\text{Be}$ ratios ($R_{26/10}$) between 1.20 ± 0.12 and 6.13 ± 0.88 (Table 1). Such depleted $R_{26/10}$ identify a burial event for all samples. Burial ages ranging from the Pliocene to the final part of the Middle Pleistocene were computed accordingly (Table 1). Pre-burial denudation rates roughly ranging from 1 to 58 m/Ma are simultaneously calculated (Table 1). We present hereafter the detail of these results, together with their 1σ uncertainties, obtained for the four different cave levels, from the highest to the lowest.

4.1. Victor cave

Very contrasting $R_{26/10}$ characterise the samples VIC1 and VIC2: 1.20 ± 0.12 and 5.72 ± 0.51 , respectively. Burial durations and pre-burial denudation rates for each sample differ accordingly: $3.28 \pm 0.22 \text{ Ma}$ and $1.44 \pm 0.24 \text{ m/Ma}$ (VIC1) versus $0.38 \pm 0.24 \text{ Ma}$ and $29.28 \pm 4.16 \text{ m/Ma}$ (VIC2).

4.2. Veronika cave

$R_{26/10}$ of the four samples collected in the main phreatic passage of the Veronika cave range from 4.20 ± 0.16 to 5.76 ± 0.32 . They yield burial durations and pre-burial denudation rates ranging from 0.26 ± 0.15 to $0.56 \pm 0.18 \text{ Ma}$ and 0.81 ± 0.07 to $20.26 \pm 2.89 \text{ m/Ma}$, respectively. At first glance, the 0.26 Ma burial age (sample VER2) may appear out of the range of the age cluster yielded by the three other samples ($\sim 0.50\text{--}0.56 \text{ Ma}$). However, the large 1σ -uncertainties associated to VER2 and 4 make burial ages of these two samples statistically indistinguishable. We therefore use the sample VER2 in further calculations. An error-weighted mean of $0.47 \pm 0.06 \text{ Ma}$ is computed

for the Veronika cave out of the four individual burial durations (removing the VER2 sample from the dataset would yield a mean burial duration of $0.51 \pm 0.07 \text{ Ma}$, not much different from the previous one).

4.3. Manants cave

$R_{26/10}$ of the four samples collected in the Manants cave at different elevations range from 2.74 ± 0.19 to 3.96 ± 0.50 . They yield burial durations and pre-burial denudation rates ranging from 1.13 ± 0.32 to $1.79 \pm 0.18 \text{ Ma}$ and 4.14 ± 0.51 to $14.15 \pm 2.65 \text{ m/Ma}$, respectively. Similar to the dataset from the Veronika cave, the 1σ -uncertainties associated to the samples (especially MAN1 and 3bis) make their individual burial ages statistically indistinguishable. An error-weighted mean of $1.59 \pm 0.10 \text{ Ma}$ is computed for the Manants cave out of the four individual burial ages.

4.4. Sainte-Anne cave

$R_{26/10}$ of the five samples collected in the Sainte-Anne cave at different elevations range from 4.05 ± 0.21 to 6.13 ± 0.88 . They yield burial ages and pre-burial denudation rates ranging from 0.24 ± 0.38 to $0.94 \pm 0.36 \text{ Ma}$ and 2.77 ± 0.30 to $58.27 \pm 11.92 \text{ m/Ma}$, respectively. Large differences are thus observed for both burial durations and pre-burial denudation rates in this cave level, yet consistent with the relative elevation of each sample (Fig. 4a). One might argue from its lower nuclide concentration values and, consequently, the larger relative uncertainty on its ^{26}Al content that sample STA2 is not as meaningful as the other samples in Sainte-Anne cave (Table 1). However, its calculated burial duration is consistent with that of STA2bis, sampled in the exact same location. As for their strongly contrasted denudation rate estimates, it is important to recall that they were calculated from single pebbles and thus refer to local denudation rather than mean catchment rates. When sedimentation occurred in the Sainte-Anne cave, the valleys had already been carved deep enough to display steep hillslopes where local denudation rates could be highly variable. We therefore consider the pair of burial duration estimates yielded by STA2 and STA2bis as significant.

5. Discussion

5.1. Relevance of the local speleogenesis in interpreting burial ages

Our burial age results clearly stress the necessity of collecting several samples in every individual cave system (Laureano et al., 2016; Sartégo et al., 2018). Indeed, although this procedure supports a robust dating of the Veronika cave at $0.47 \pm 0.06 \text{ Ma}$, it was also absolutely required to uncover potential methodological or geomorphic issues in the other cave levels (Häuselmann and Granger, 2005; Dunai, 2010).

5.1.1. Contamination by younger material

The ~ 0.4 and 3.3 Ma burial ages obtained for the Victor cave diverge by one order of magnitude. This large discrepancy most probably results from the distinct positions of the sampling sites within the cave. Whereas the VIC1 sample was collected in the lower main development of the cave at $\sim 125 \text{ m}$ relative elevation, the VIC2 sample was located much nearer to the cave entrance, directly at the bottom of the uppermost underground shaft ($\sim 135 \text{ m}$ relative elevation). At such high position above the present Ourthe River, the $0.38 \pm 0.24 \text{ Ma}$ burial age is without doubt geomorphologically inconsistent. In particular, it strongly contradicts the robust ^{10}Be depth profile dating of the YMT at Colonster, which provided an age of $\sim 0.4 \text{ Ma}$ for terrace deposits located 80 m below the level of the Victor cave (Rixhon et al., 2011). We thus interpret the anomalous young age of VIC2 as indicating a

later reactivation of the sinkhole (now in interfluvial position) and injection of younger sediments into the oldest karstic level of the Chawresse system. Moreover, assuming a gravitational collapse of unknown thickness, it is unsure whether the material originates from the surface or the sub-surface and, thereby, whether the initial $R_{26/10}$ of this sample does not violate the key assumption for burial dating (see Section 3 above). Consequently, the VIC2 sample is discarded and we consider the Late Pliocene burial age of VIC1 to be representative of the time when the water table (and the Ourthe River) existed at these high elevations.

5.1.2. Probable intra-karstic reworking

The four Early Pleistocene burial ages of the Manants cave at less than 35 m relative elevation must mandatorily be addressed against the background of progressive river downcutting over the Plio-Quaternary. Based on the mid-Middle Pleistocene age of the YMT at Colonster (and, more broadly, also elsewhere in the Meuse catchment; Rixhon et al., 2011), they are substantially older than expected at such a low relative elevation. Three explanatory hypotheses may be examined, namely an alternative model of speleogenesis, a previous burial episode of the sampled material or an intra-karstic reworking with downward motion.

An alternative *per ascensum* model of speleogenesis, such as the one documented in the Ardèche Valley (e.g., Tassy et al., 2013), would contradict all geomorphic evidence of stepwise base-level lowering and incision in the entire Ardennian Meuse River network related to Quaternary uplift (e.g., Juvigné, 1979; Pissart et al., 1997; Demoulin et al., 2012; Rixhon and Demoulin, 2018). In the lower Ourthe Valley, the well-preserved terrace staircase and its geomorphological coupling with cave systems strongly point to a *per descensum* model of speleogenesis (Harmand et al., 2018). The latter is acknowledged not only for the Chawresse system (Ek, 1961; Cornet, 1995) but also for the newly discovered Noû Bleû cave located several kilometers upstream (Peeters and Ek, 2018). The hypothesis of an alternative speleogenetic model is thus highly unlikely.

Even if no direct evidence precludes the possibility that some of the sampled material underwent a burial episode before entering the karstic system, two lines of argument point to intra-karstic reworking as the most likely cause of the ages that are too old. First, beyond exhibiting higher depletion than the Veronika samples (Table 1), the Manants $R_{26/10}$ data subset is internally consistent, with the lowest variability among all cave levels. This points to a single burial history for all Manants samples, and thus most likely an exclusively intra-karstic history. Indeed, reworking of pebbles that would have experienced subaerial burial events before entering the cave system (e.g., at the base of thick Early Pleistocene Ourthe terrace deposits) would probably have implied a large scatter in the depleted $R_{26/10}$ (different burial durations and depths).

Second, the intricate karstic system of the Manants cave dominated by vadose shafts (Fig. 4) points to multiphase speleogenetic processes (De Bie, 2013), which probably also entailed a complex underground evolution of the cave sedimentary infill. Following De Bie (2013),

who considers that the Chawresse and Veronika caves form a single system, we thus suggest that the Chawresse/Veronika and the Manants/Sainte-Anne systems evolved independently, possibly also with some temporal overlap that might explain the complex underground topography of the Manants cave and the Early Pleistocene burial ages obtained for its cave infill. A realistic, though speculative, history of the Manants samples might have implied the following stages: (i) washing of sediments into dolines and/or sinkhole shafts in the vadose zone above an Early Pleistocene stability level, with substantial shielding to cosmic rays already allowing some $R_{26/10}$ decrease; (ii) from the late Early Pleistocene, progressive base-level lowering and Ourthe and Chawresse incision promoting downward development of the shafts and travel of the trapped sediments, possibly aided by piping and underground drainage, to depths possibly beyond reach of the cosmic rays; (iii) Middle Pleistocene stability phase inducing the independent formation and infilling of the phreatic tubes of the Veronika cave whilst the Manants clasts remained buried in their separate system; (iv) later in the Middle Pleistocene, main phase of river downcutting and renewed downward displacement of the sediments buried in the Manants cave, however, not affecting the fossilized Veronika tubes and their infill; (v) probably in connection with the main tube formation in the Sainte-Anne cave sometime during the late Middle Pleistocene, phreatic overprinting of the Manants cave with essentially lateral reworking bringing the clasts in their sampling position. Note that the same reasoning can be held for the older burial ages of sediments sampled in the higher phreatic tubes of Sainte-Anne, which might indicate input of older material through the Manants cave as a siphon connects both caves (Fig. 4; De Bie, 2013).

Several field observations support this scenario. A dense network of well-developed dolines (depth locally > 10 m) occur directly to the south of the cave (“*dolines syncline*”, Fig. 7a). Located upslope south of the Chawresse Valley at elevations of 180–200 m, they display active sinkholes and sediment accumulation at their bottom (Fig. 7b). Although their possible hydrological connection with the Manants cave has not been explored so far (De Bie, 2013), we may postulate that similar extended vertical connection between the ground surface and deeper cave levels also existed in the past. Moreover, in contrast with all other caves of the Chawresse system, the current Manants cave's entrance corresponds to an active sinkhole in the sub-aerial Chawresse streambed. Active drainage of the cave's vadose shafts by the underground stream obviously still facilitates the downward transport of clastic material (Fig. 7c). For all these reasons, we interpret all burial ages obtained for the Manants samples and those of STA1, 1bis and 4 in Sainte-Anne as discordant data telling corollary events of the drainage system downcutting.

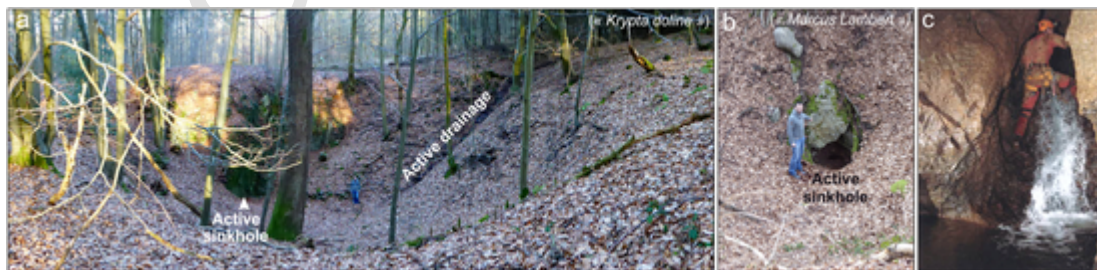


Fig. 7. a & b. Series of well-developed, active dolines/sinkholes located atop the southern hillslope of the Chawresse Valley southward of the Manants cave (see location in Fig. 3a; photos: G. Rixhon). c. Active vertical drainage (i.e., underground Chawresse stream) in vadose conditions in the Manants cave (photo: P. De Bie).

5.2. Comparison of the burial ages with Neogene/Quaternary fluvial deposits

5.2.1. Pre-Quaternary fluvial evolution at the northern rim of the massif

The 3.28 ± 0.22 Ma burial age in the Victor cave represents the first Pliocene numerical age for fluvial deposits located within the Ardennian Meuse catchment. This age is consistent with the position of the Victor cave at the plateau's margin atop the eastern Ourthe Valley side (Fig. 4) and the Neogene age assigned to the lowest beveled surfaces flanking the incised Quaternary valleys (Demoulin, 1995; Demoulin et al., 2018). Moreover, the dated deposit lies at a lower elevation than the quartz- and quartzite-rich fluvial gravels discontinuously covering the Ourthe/Meuse interfluvium 155 to 180 m above the modern valley bottoms (e.g., Rixhon and Demoulin, 2010; Fig. 8a). Located ~5 km to the northwest of the Chawresse multi-level system (Fig. 1b), these gravels, locally known as “Graviers Liégeois” (Pissart, 1964), have been interpreted as the oldest Ardennian River sediments deposited by a proto-Ourthe system and tentatively dated from the Miocene (Supplementary material 4), based on stratigraphic and pedogenetic evidence (Buurman, 1972) (Fig. 8a). Finally, although the highest terrace remnants in the lower Ourthe Valley hardly reach 125 m relative elevation (Cornet, 1995), the oldest terrace deposits of the Meuse in the nearby Liege area, traditionally referred to as “kieseloolite terraces” (Macar, 1975; Supplementary material 4), occur within the same range of relative elevation as the Victor cave (~115–135 m) (Fig. 8a) (Juvigné and Renard, 1992; Rixhon and Demoulin, 2018). Despite the lack of direct numerical age of the kieseloolite terraces, authors now agree that their stratigraphic correlation with the Kieseloolite Formation in the Roer Valley Graben dates them between the Late Tortonian and the Early Piacenzian (Westerhoff et al., 2008; Rixhon and Demoulin, 2018; Beerten et al., 2018; Munsterman et al., 2019). Overall, the Pliocene burial age of the Victor cave thus appears in good agreement with the available geomorphic and sedimentary evidence in the area.

5.2.2. Geomorphological and chronological link between the Veronika cave and the YMT

Our convergent burial durations in the main phreatic tubes of the Veronika cave point to a long-lasting regional base level ~70–75 m above the current valley bottom around 0.47 Ma. At this elevation, the cave lies 15–20 m above the YMT of the Ourthe (Fig. 9). The ^{10}Be depth profile performed in the YMT sediments at Colonster, 3 km

downstream of the Chawresse cave system, reliably dated the terrace abandonment time at ~0.39 Ma (Rixhon et al., 2011), which is at first glance in perfect agreement with the ~0.5 Ma age of the Veronika cave level.

However, the story is somewhat more complex. First, in the lower Meuse ~20 km north of Liege, the abandonment time of the Romont terrace, formerly correlated to the YMT (Juvigné, 1992), was dated at 0.73 ± 0.12 Ma via a twofold ^{10}Be and ^{26}Al depth profile (Rixhon et al., 2011). The later reassignment of this terrace to the next higher level within the Main Terrace Complex led Rixhon and Demoulin (2018) to propose a younger age around 0.62 Ma for the YMT abandonment time in this valley reach. Second, ~20 km upstream of the Chawresse area, another ^{10}Be depth profile in terrace deposits of the Amblève River close to its confluence with the Ourthe (Fig. 1b) revealed that, although the YMT was abandoned at 0.22 ± 0.03 Ma in that place, it had started to aggrade much earlier, around 0.58 Ma (Rixhon et al., 2011). Broadly consistent with the YMT age at Romont, the latter age thus implies that the lower Ourthe River had also already incised its valley down to slightly less than 55 m of relative elevation (i.e., the base of the YMT) around 0.58–0.62 Ma. This seems to contradict the younger 0.47 ± 0.06 Ma mean burial age obtained in the higher-located Veronika cave.

This apparent discrepancy finds its explanation in the location of the Veronika cave in the Chawresse Valley, about 800 m upstream of the Ourthe confluence, which, at YMT time, was approximately superposed to the present one. Therefore, we interpret the 15–20 m elevation difference between the cave and the Ourthe YMT as expressing the hydraulic gradient beneath the hillslopes east of the Ourthe at YMT time. This ~2.5% gradient is very close to the 2.5–3% westward slope of the Veronika main galleries (Fig. 9) and the ~3% slope of the sub-aerial channel in the upper Chawresse inherited from the Early Pleistocene, the Middle Pleistocene incision wave having not reached the upper Chawresse (Beckers et al., 2015). So connecting the Veronika cave, and thus making it contemporaneous, with the Ourthe YMT is geomorphically and chronologically consistent. Once the Ourthe River had started to develop its YMT floodplain sometime between 0.62 and 0.58 Ma, the Veronika karstic level in turn began to form following the hydraulic gradient of the time. Clasts sampled in the upper part of a ~2-m thick deposit date the later filling of its galleries around 0.47 Ma, i.e., well before the YMT level was abandoned through renewed Ourthe incision around 0.39 Ma in this area (Rixhon et al., 2011). We also note that the YMT time was the last long period (including the long warm MIS11) of stability of the river before the Late Pleistocene, so

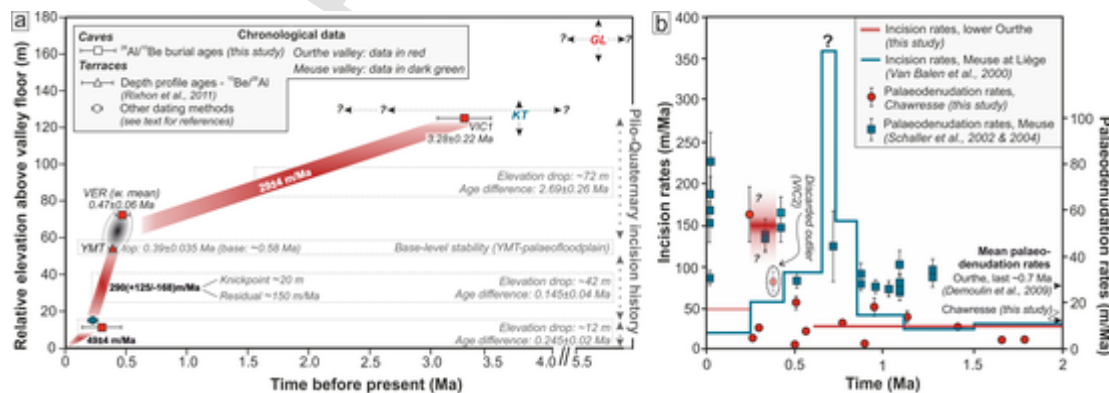


Fig. 8. Long-term fluvial landscape evolution at the northern rim of the Ardennes in the main trunk (Meuse) and its main tributary (Ourthe). a. Computation of Plio-Quaternary incision rates based on the $^{26}\text{Al}/^{10}\text{Be}$ burial ages from this study and from compilation of existing ages (see references in figure insert and text). Note the one order magnitude change in the Ourthe Valley and the sustained incision pulse recorded during the Middle Pleistocene. GL (i.e., oldest proto-Ourthe deposits) and KT (i.e., oldest Meuse terraces) refer to Neogene/Quaternary fluvial deposits located in Fig. 1b. Vertical and horizontal dashed black arrows refer to their elevation range and supposed time range (with question marks), respectively. b. Compilation of incision and palaeodenudation rates. Note that the incision pulse in the lower Ourthe occurred later than the incision peak in the main trunk, which is characterized by questionable very high rates (>350 m/Ma, see text). As for the discarded outlier, see text for further information. Age uncertainties relative to palaeodenudation data are not provided for a matter of clarity.

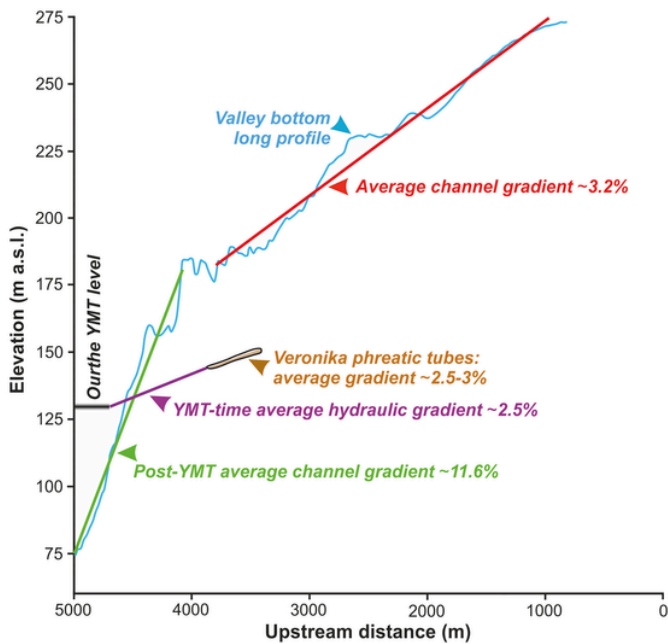


Fig. 9. Morphometric characteristics of the Chawresse tributary (note the well-marked hanging valley sensu Wobus et al., 2006) and gradient relationship between the Veronika Cave and the Ourthe YMT level.

that one could a priori expect it would have been favourable to such a large karstic development as that of the Veronika cave.

5.3. Incision rate variability over the Plio-Quaternary

The ^{10}Be -based ages obtained by Rixhon et al. (2011, 2014) for YMT remnants in the lower Meuse – lower Ourthe – Amblève system provided first constraints on the long-term incision history in N. Ardennes. Not only does the present study confirm them but it also yields the first numerical age for one of the highest attested levels of the Plio-Quaternary downcutting of the Ardennian drainage network. With the Pliocene age of the landscape level in which the Victor cave formed, it brings quantitative support to the long-held assumption of contrasted incision rates between the Pliocene and Early Pleistocene on one hand, the Middle Pleistocene to present on the other hand (Fig. 8a–b).

Based on the differences between the VIC1 sample and the YMT base in the lower Ourthe in terms of relative elevation (125 m vs ~49 m, for 6 m thick YMT deposits) and age (3.28 Ma vs. 0.58 Ma), the Late Pliocene and the Early Pleistocene were characterized by a mean incision rate of 29 ± 4 m/Ma (Fig. 8a). Then, a period of stability occurred from 0.62–0.58 to 0.39 Ma (i.e., the lifetime of the YMT as a floodplain in the lower Ourthe Valley, see also Rixhon et al., 2014). The next period over which an average incision rate may be calculated is framed by the time of abandonment of the YMT and a set of dates pointing to a relative elevation of 12 m for the Ourthe level in the late Middle Pleistocene. The latter timing is first indicated by the two samples (STA2 and STA2bis) dating the youngest phase of activity in the main phreatic tube of Sainte-Anne (12 m relative elevation) between 0.24 and 0.3 Ma, though with penalizing large age uncertainties (Table 1). Second, 40 km farther downstream, the interglacial deposits capping the Caberg terrace of the Meuse at 15–18 m relative elevation in the Belvédère site near Maastricht have been consistently dated at 0.25 ± 0.02 Ma by thermoluminescence on burned flints and 0.22 ± 0.04 Ma by ESR on mollusc shells (Huxtable, 1993; Van Kolf-schoten et al., 1993). We thus calculate a weighted mean age of the Sainte-Anne – Caberg level of 0.245 ± 0.02 Ma. Based on a difference in elevation of 42 m, an average incision rate of $290(+125/-68)$ m/

Ma between 0.39 ± 0.04 and 0.245 ± 0.02 Ma is inferred. However, beyond the fact that it confirms the strong acceleration of incision from the Middle Pleistocene onwards (Demoulin and Hallot, 2009; Rixhon et al., 2011), the meaning of this rate is not straightforward because it incorporates two fundamentally different components. They are (i) the delayed upstream propagation of an approximately 20-m high wave of erosion responding to a tectonic uplift pulse in the early Middle Pleistocene and travelling along the lower Ourthe around 0.39 Ma (Demoulin et al., 2012; Beckers et al., 2015), and (ii) a slower continued incision over the rest of the period (Fig. 8a). Subtracting the 20 m amount of incision propagated with the erosion wave leaves a residual post-knickpoint average incision rate in the order of 150 m/Ma as a direct response to the late Middle Pleistocene uplift of the area, still much larger than the Pliocene-Early Pleistocene rate. Finally, according to the same data, the mean incision rate since 0.245 ± 0.02 Ma would fall in the range of 45–53 m/Ma. This is in agreement with the rougher 33–81 m/Ma estimation derived from the presence of the 74–90 ka old Rocourt tephra (Poucllet et al., 2008) in low terraces (~3 m relative elevation) of the Ourthe and the Amblève, as well as its absence in the next higher terrace of the Amblève at 6 m relative elevation (Juvigné, 1973, 1979; Rixhon and Demoulin, 2010).

These long-term incision rates can be compared with those compiled by Van Balen et al. (2000) for the Meuse at Liège based on a reinterpretation of palaeomagnetic data previously obtained in the terrace staircase of the lower Meuse near Maastricht (Van den Berg, 1996) (Fig. 8b). We recall, however, that the chronological interpretation of these palaeomagnetic data, especially those collected from the main terrace complex, has long been a matter of debate (Van Balen et al., 2000; Westaway, 2002; Rixhon and Demoulin, 2010; Rixhon et al., 2011). Nevertheless, the general picture remains valid, with low incision rates in the Early Pleistocene, a major rate increase in the first half of the Middle Pleistocene, followed by a progressive decrease of the rates since the late Middle Pleistocene (Fig. 8b). We also note the different timing of maximum incision between the lower Ourthe - Chawresse area and the lower Meuse. The latter is related to the time the Middle Pleistocene erosion wave needed to propagate into the Ardennian drainage system, causing delayed knickpoint passage and valley incision in the Ourthe with respect to the Meuse (Rixhon et al., 2011; Demoulin et al., 2012; Rixhon and Demoulin, 2018) (Fig. 8b). Finally, as for the reduced incision rates observed in both the Meuse and Ourthe since ~0.25 Ma, one may tentatively link them to the loss of drainage area (~3400 km²), and thus stream power, suffered by the Meuse because of the capture of the upper Moselle at the time of the Caberg terrace (e.g., Pissart et al., 1997), even though the numerical age of the capture is still debated (Cordier et al., 2013).

5.4. Palaeodenudation rates

Besides burial durations in the Chawresse karstic system, the measured $R_{26/10}$ yield pre-burial denudation rates ranging from 0.8 to 58.3 m/Ma (Table 1), adding information to the existing database used to infer basin denudation rates in the Ardennes (Schaller, 2002, 2004; Demoulin et al., 2009). However, we first stress two main limitations of our rate data. First, as our samples consist of single or a few amalgamated quartz or quartzite clasts, the derived rates do not refer to mean basin denudation but rather to local erosion under the topographic conditions of the places wherefrom the samples come within the area of outcropping siliceous rocks (in the upstream Chawresse catchment). Second, most of the calculated rates concern the period of slow denudation from the Pliocene to the early Middle Pleistocene, before the post-YMT erosion wave had reached the study area, and only two samples (STA2 and STA2bis) provide scarce information about the younger times of assumed higher erosion.

All our rate estimates predating the time of rapid post-YMT incision, i.e., those obtained from the Victor, Manants, and Veronika caves but also those of Sainte-Anne with burial ages older than 0.39 Ma, were expected to reflect a smoothly undulating fluvial landscape with gentle slopes and low relief, drained by wide shallow valleys. Indeed, denudation rate increases from a very low 1.44 ± 0.24 m/Ma at ~ 3.3 Ma in the Early Piacenzian (sample VIC1) to a weighted mean of 7.53 ± 0.26 m/Ma between 2 and 1 Ma (Manants cave samples), 9.19 ± 0.46 m/Ma between 1 and 0.8 Ma (samples STA1, 1bis and 4), and 7.45 ± 0.22 m/Ma around 0.5 Ma (Veronika cave samples). Note that, because of the dependence of the error on the value of the denudation rate, mean rates have been obtained here from weighting the data by their associated relative error instead of their variance. In each of these periods, the spread of individual clast denudation estimates remains limited, with maximal values always ≤ 20 m/Ma, confirming low to moderate denudation of a hardly incised landscape of Neogene planation surfaces in the lower Ourthe area (Demoulin et al., 2018). By contrast, though clearly needing confirmation by further measurements, the two samples attesting denudation after the post-YMT erosion wave had reached the study area and enhanced river incision had begun (STA2 and 2bis) show higher and more variable rates, consistent with a greater relief and steeper valley slopes.

At a regional scale, Schaller et al. (2004) provided mean palaeodenudation rates for the Ardennian Meuse basin based on ^{10}Be measurements from different terrace deposits of approximately known ages located in the Maastricht area and spanning the period since 1.3 Ma. They increase from $\sim 25\text{--}35$ m/Ma in the Early Pleistocene to $\sim 40\text{--}80$ m/Ma since the beginning of the Middle Pleistocene. As the authors acknowledged, these rates suffer from uncertainties. They are linked (i) to poor age constraints on many sampled terrace deposits and (ii) to the limited adequacy of the sampled material in representing all parts of the catchment, be it because carbonate rock areas do not deliver quartz to the rivers or the 0.5–1 mm grain size fraction on which the ^{10}Be measurements were made is hardly present in some sediments e.g., the kaolinic weathering products mantling large plateau areas of the Ardennes. Nevertheless, they compare well with the local denudation data presented here. Indeed, the pre-0.7 Ma rates of 25–35 m/Ma obtained by Schaller et al. (2004) refer to the Meuse catchment upstream of Maastricht and thus incorporate a non-negligible component of valley downcutting and widening in the main branches of the river system. The fact that this component of valley development is almost absent in the source area of our samples, namely the hardly eroded upstream part of the small Chawresse catchment, readily explains the lower rates in the order of 7–10 m/Ma they yielded.

Finally, based on eroded volumes estimated from geomorphic arguments for interfluvies in the Condroz area, to which the Chawresse upper catchment may be likened, Demoulin et al. (2009) also obtained denudation rates in the order of 5–10 m/Ma in the Pliocene and Early Pleistocene. Interestingly, despite not being aimed at high-resolution evaluation of denudation, the recently published study of apatite fission track data from northern Ardennes comes to the similar conclusion that denudation was very slow in this area in the Neogene (Barbarand et al., 2018). As for the more recent increased denudation rates, we only note that the rate of ~ 58 m/Ma yielded by sample STA2 originating from a still now not much incised area is in line with the catchment-wide rates between 40 and 80 m/Ma calculated by Schaller et al. (2004). It also agrees well with local denudation data in the same range obtained from interfluvies in two small catchments of the Black Forest (Meyer et al., 2010). Finally, the Chawresse denudation rates present first hints that the timing of the Middle Pleistocene increase in denudation rate in the Ardennes might be linked to the arrival of the post-YMT erosion wave in any particular catchments, being thus more tectonically than climatically triggered.

6. Conclusion

Though facing limitations inherent to $^{26}\text{Al}/^{10}\text{Be}$ burial dating of ancient alluvium-filled karstic passages, this study demonstrates the usefulness of the approach to unravel the main episodes of fluvial base-level stability in the Ardennes during the Plio-Quaternary. Its main outcomes are threefold. First, the Early Pleistocene burial ages of the Manants cave most probably reflect an uncoupled speleogenesis with respect to the higher-lying phreatic tubes of Veronika and Chawresse (mean burial age around 0.5 Ma). These discordant ages stress the necessity for sampling only well-developed alluvium-filled phreatic tubes, where contamination from higher levels appears unlikely (e.g., the Veronika cave), to provide reliable long-term incision rates. Second, the computed burial ages from the Victor and Veronika caves, together with the reliable abandonment time of the YMT in the lower Ourthe (Rixhon et al., 2011), quantitatively attest for the first time the long-held assumption of contrasted incision rates between the Pliocene-Early Pleistocene and the Middle Pleistocene-present. At ~ 0.39 Ma, the Middle Pleistocene rates increased transiently from ~ 30 to ~ 150 m/Ma. The long-term incision history in the lower Ourthe exhibit a similar pattern to that in the lower Meuse, although the peak incision episode, in good concordance with previous studies (e.g., Rixhon et al., 2011; Demoulin et al., 2012), occurred later in the tributary. This results from the delayed upstream propagation of the Middle Pleistocene erosion wave, itself triggered by the main tectonic uplift pulse of the early Middle Pleistocene. Third, despite their limitations, palaeodenudation rates inferred in the Chawresse catchment are fairly consistent with other long-term denudation data.

We, however, finally state that further dating efforts are required to understand better the complex response of the Meuse drainage system to coupled tectonic and climatic forcings over the Plio-Quaternary. Whilst the well-preserved Ardennian terrace sequences obviously represent a favourable setting, this study highlights the usefulness of alluvium-filled multi-level cave systems to unravel the long-term history of river incision. Other multi-level systems occur along the Meuse (e.g., Monfat cave; Quinif, 2002) and some tributaries, namely the Ourthe (e.g., Nôû Bleû; Peeters and Ek, 2018), and the Lesse (e.g., Han-sur-Lesse; Quinif and Hallet, 2018); they should be thoroughly investigated in that respect in the near future.

Uncited references

Boenigk and Frechen, 2006
Crosby and Whipple, 2006
Mudelsee and Schulz, 1997
Nishiizumi, 2004

Declaration of competing interest

We wish to confirm that there are no known conflicts of interest associated with this publication and there has been no significant financial support for this work that could have influenced its outcome.

Acknowledgments

We warmly thank Paul de Bie (caver) and Camille Ek (caver and karst expert) for their helpful support during cave exploration and sampling as well as for sharing their exceptional field knowledge of the spectacular Chawresse multi-level cave system. More generally, all caver associations, which contributed to the progressive discovery of this imposing cave system, are acknowledged here. We also thank Yannick Levecq and Stéphane Jaillet for the support during exploration and fruitful discussion, respectively. The ASTER AMS national facility (CEREGE, Aix en Provence) is supported by the INSU/CNRS, the ANR through the “Projets thématiques d'excellence” program for the

“Equipements d'excellence” ASTER-CEREGE action and IRD. We also thank Zsófia Ruszkiczay-Rüdiger and one anonymous reviewer for their insightful comments.

Appendix A. Supplementary data

Supplementary data to this article can be found online at <https://doi.org/10.1016/j.geomorph.2020.107424>.

References

- Alexandre, J., 1976. Les surfaces de transgression exhumées et les surfaces d'aplanissement. In: Pissart, A. (Ed.), *Géomorphologie de la Belgique*, Lab. Géol. Et Géogr. Phys., Univ. Liège, Liège. pp. 75–92.
- Anthony, D., Granger, D., 2007. A new chronology for the age of Appalachian erosional surfaces determined by cosmogenic nuclides in cave sediments. *Earth Surf. Process. Landf.* 32, 874–887. doi:10.1002/esp.
- Arnold, M., Merchel, S., Bourles, D.L., Braucher, R., Benedetti, L., Finkel, R.C., Aumaitre, G., Gottang, A., Klein, M., 2010. The French accelerator mass spectrometry facility ASTER: improved performance and developments. *Nuclear Instruments and Methods in Physics Research B: Beam Interactions with Materials and Atoms* 268, 1954–1959.
- Barbarand, J., Bour, I., Pagel, M., Quesnel, F., Delcambre, B., Dupuis, C., Yans, J., 2018. Post-Paleozoic evolution of the northern Ardenne Massif constrained by apatite fission-track thermochronology and geological data. *BSGF-Earth Sciences Bulletin* 189, 1–16. doi:10.1051/bsgf/2018015.
- Bastin, G., Quinif, Y., Dupuis, C., Gascoyne, M., 1988. La séquence sédimentaire de la grotte de Bohon (Belgique). *Ann. Soc. Geol. Belg.* 111, 51–60.
- Beckers, A., Bovy, B., Hallot, E., Demoulin, A., 2014. Controls on knickpoint migration in a drainage network of the moderately uplifted Ardennes Plateau, Western Europe. *Earth Surf. Process. Landf.* 40, 357–374. doi:10.1002/esp.3638.
- Boenigk, W., Frechen, M., 2006. The Pliocene and Quaternary fluvial archives of the Rhine system. *Quat. Sci. Rev.* 25, 550–574. doi:10.1016/j.quascirev.2005.01.018.
- Borchers, B., Marrero, S., Balco, G., Caffee, M., Goehring, B., Lifton, N., Nishiizumi, K., Phillips, F., Schaefer, J., Stone, J., 2016. Geological calibration of spallation production rates in the CRONUS-Earth project. *Quat. Geochronol.* 31, 188–198. doi:10.1016/j.quageo.2015.01.009.
- Bovy, B., Braun, J., Demoulin, A., 2016. Soil production and hillslope transport in mid-latitudes during the last glacial-interglacial cycle: a combined data and modelling approach in northern Ardennes. *Earth Surf. Process. Landf.* 41, 1758–1775.
- Braucher, R., Merchel, S., Borgomano, J., Bourlès, D.L., 2011. Production of cosmogenic radionuclides at great depth: a multi element approach. *Earth Planet. Sci. Lett.* 309, 1–9. doi:10.1016/j.epsl.2011.06.036.
- Brown, E.T., Edmond, J.M., Raisbeck, G.M., Yiou, F., Kurz, M.D., Brook, E.J., 1991. Examination of surface exposure ages of Antarctic moraines using in-situ produced ^{10}Be and ^{26}Al . *Geochim. Cosmochim. Acta* 55, 2269–2283.
- Buurman, P., 1972. *Paleopedology and Stratigraphy of the Condrusian Penplain (Belgium)* - Centre for Agricultural Publishing and Documentation Wageningen.
- Chmeleff, J., Von Blanckenburg, F., Kossert, K., Jakob, D., 2010. Determination of the ^{10}Be half-life by multicollector ICP-MS and liquid scintillation counting. *Nuclear Instruments and Methods in Physics Research B: Beam Interactions with Materials and Atoms* 268, 192–199.
- Cloetingh, S., Ziegler, P.A., Beekman, F., Andriessen, P.A.M., Matenco, L., Bada, G., Garcia-Castellanos, D., Hardebol, N., Dezès, P., Sokoutis, D., 2005. Lithospheric memory, state of stress and rheology: neotectonic controls on Europe's intraplate continental topography. *Quat. Sci. Rev.* 24, 241–304. doi:10.1016/j.quascirev.2004.06.015.
- Cordier, S., Frechen, M., Harmand, D., 2013. Dating fluvial erosion: fluvial response to climate change in the Moselle catchment (France, Germany) since the Late Saalian. *Boreas* 43, 450–468 (ISSN 0300-9483). doi:10.1111/bor.1205.
- Cornet, Y., 1995. L'encaissement des rivières ardennaises au cours du Quaternaire. In: Demoulin, A. (Ed.), *L'Ardenne, Essai de Géographie Physique*, Liège. pp. 155–177.
- Crosby, B.T., Whipple, K.X., 2006. Knickpoint initiation and distribution within fluvial networks: 236 waterfalls in the Waipaoa River, North Island, New Zealand. *Geomorphology* 82, 16–38. doi:10.1016/j.geomorph.2005.08.023.
- Davis, W.M., 1895. La Seine, la Meuse et la Moselle. *Ann. Géog.* 4, 25–49.
- De Bie, P., 2013. Le système Chawresse-Veronika et la vallée de la Chawresse. *Union Belge de Spéléologie* (161 p).
- Demoulin, A., 1995. Les surfaces d'érosion méso-cénozoïques en Ardenne-Eifel. *Bull. Soc. Géol. France* 166 (5), 573–585.
- Demoulin, A., Hallot, E., 2009. Shape and amount of the Quaternary uplift of the western Rhenish shield and the Ardennes (western Europe). *Tectonophysics* 474, 696–708. doi:10.1016/j.tecto.2009.05.015.
- Demoulin, A., Hallot, E., Rixhon, G., 2009. Amount and controls of the Quaternary denudation in the Ardennes massif (western Europe). *Earth Surf. Process. Landf.* 34, 1487–1496. doi:10.1002/esp.1834.
- Demoulin, A., Beckers, A., Rixhon, G., Braucher, R., Bourlès, D., Siame, L., 2012. Valley downcutting in the Ardennes (W Europe): interplay between tectonically triggered regressive erosion and climatic cyclicity. *Netherlands Journal of Geosciences — Geologie En Mijnbouw* 91 (2), 79–90.
- Demoulin, A., Barbier, F., Dekoninck, A., Verhaert, M., Ruffet, G., Dupuis, C., Yans, J., 2018. Erosion surfaces in the Ardenne-Oesling and their associated kaolinic weathering mantle. In: Demoulin, A. (Ed.), *Landscapes and Landforms of Belgium and Luxembourg*. Springer, pp. 63–84.
- Dubois, C., Quinif, Y., Baele, J., Barriquand, L., Bini, A., Bruxelles, L., Dandurand, G., Havron, C., Kaufmann, O., Lans, B., Maire, R., Rodet, J., Rowberry, M.D., Tognini, P., Vergari, A., 2014. The process of ghost-rock karstification and its role in the formation of cave systems. *Earth Sci. Rev.* 131, 116–148.
- Ek, C., 1957. Les terrasses de l'Ourthe et de l'Amblyve inférieures. *Ann. Soc. Geol. Belg.* 80, 333–353.
- Ek, C., 1961. Conduits souterrains en relation avec les terrasses fluviales. *Ann. Soc. Geol. Belg.* 84, 313–340.
- Ek, C., Poty, E., 1982. Esquisse d'une chronologie des phénomènes karstiques en Belgique. *Revue Belge de Géographie* 1, 73–85.
- Farrant, A.R., 2004. Paragenesis. In: Gunn, J. (Ed.), *Encyclopedia of Caves and Karst Science*. Fitzroy Dearborn, New York, pp. 569–571.
- Granger, D.E., 2006. A review of burial dating methods using ^{26}Al and ^{10}Be . *Geol. Soc. Am. Spec. Pap.* 415, 1–16.
- Granger, D.E., 2014. Cosmogenic nuclide burial dating in archaeology and paleoanthropology. In: *Treatise on Geochemistry*, Elsevier, 2nd ed. Elsevier Ltd., pp. 81–97. doi:10.1016/B978-0-08-095975-7.01208-0.
- Granger, D.E., Kirchner, J.W., Finkel, R.C., 1997. Quaternary downcutting rate of the New River, Virginia, measured from differential decay of cosmogenic ^{26}Al and ^{10}Be in cave-deposited alluvium. *Geology* 25, 107–110. doi:10.1130/0091-7613(1997)025<0107.
- Harmand, D., Adamson, K., Rixhon, G., Jaillet, S., Losson, B., Devos, A., Hez, G., Calvet, M., Audra, P., 2017. Relationships between fluvial evolution and karstification related to climatic, tectonic and eustatic forcing in temperate regions. *Quat. Sci. Rev.* 166, 38–56. doi:10.1016/j.quascirev.2017.02.016.
- Häuselmann, P., Granger, D.E., 2005. Dating of caves by cosmogenic nuclides: method, possibilities, and the Siebenhengste example (Switzerland). *Acta Carsologica* 34, 43–50.
- Juvigné, E., 1973. Datation de sédiments quaternaires à Tongrinne et à Tilff par des minéraux volcaniques. *Ann. Soc. Géol. Belg.* 96, 411–412.
- Juvigné, E., 1979. L'encaissement des rivières ardennaises depuis le début de la dernière glaciation. *Z. Geomorphol.* 23, 291–300.
- Juvigné, E., Renard, F., 1992. Les terrasses de la Meuse de Liège à Maastricht. *Ann. Soc. Geol. Belg.* 115, 167–186.
- Korschinek, G., Bergmaier, A., Faestermann, T., Gerstmann, U.C., Knie, K., Rugel, G., Wallner, A., Dillmann, I., Dollinger, G., Lieser Von Gostomski, C., Kossert, K., Maiti, M., Poutivsev, M., Remmert, A., 2010. A new value for the half-life of ^{10}Be by heavy-ion elastic recoil detection and liquid scintillation counting. *Nuclear Instruments and Methods in Physics Research B: Beam Interactions with Materials and Atoms* 268, 187–191.
- Laureano, F.V., Karmann, I., Granger, D.E., Auler, A.S., Almeida, R.P., Cruz, F.W., Stricks, N.M., Novello, V.F., 2016. Geomorphology two million years of river and cave aggradation in NE Brazil: implications for speleogenesis and landscape evolution. *Geomorphology* 273, 63–77. doi:10.1016/j.geomorph.2016.08.009.
- Macar, P., 1975. L'évolution quaternaire des bassins fluviaux de la mer du Nord méridionale. *Soc. Géol. Belg.* Liège (318 p).
- Merchel, S., Bremser, W., 2004. First international ^{26}Al interlaboratory comparison – part I. *Nuclear Instruments and Methods in Physics Research B: Beam Interactions with Materials and Atoms* 223–224, 393–400.
- Merchel, S., Hergers, U., 1999. An update on radiochemical separation techniques for the determination of long-lived radionuclides via accelerator mass spectrometry. *Radiochim. Acta* 84 (4), 215–219. doi:10.1524/ract.1999.84.4.215.
- Merchel, S., Arnold, M., Aumaitre, G., Benedetti, L., Bourlès, D.L., Braucher, R., Alfimov, V., Freeman, S.P.H.T., Steier, P., Wallner, A., 2008. Towards more precise ^{10}Be and ^{36}Cl data from measurements at the 10^{-14} level: influence of sample preparation. *Nuclear Instruments and Methods in Physics Research B: Beam Interactions with Materials and Atoms* 266, 4921–4926.
- Meyer, W., Stets, J., 1998. Junge Tektonik im Rheinischen Schiefergebirge und ihre Quantifizierung. *Z. Dtsch. Ges. Geowiss.* 149, 359–379.
- Meyer, W., Albers, H., Berners, H., von Gehlen, K., Glatthaar, D., Löhnertz, W., Pfeffer, K., Schnütgen, A., Wienecke, K., Zakosek, H., 1983. Pre-Quaternary uplift in the central part of the Rhenish massif. In: Fuchs, K., von Gehlen, K., Mälzer, H., Murawski, H., Semmel, A. (Eds.), *Plateau Uplift. The Rhenish Shield – A Case History*. Springer, Berlin, pp. 39–46.
- Meyer, H., Hetzel, R., Fügenshuh, B., Strauss, H., 2010. Determining the growth rate of topographic relief using in-situ produced ^{10}Be : a case study in the Black Forest, Germany. *Earth Planet. Sci. Lett.* 290, 391–402. doi:10.1016/j.epsl.2009.12.034.
- Mudelsee, M., Schulz, M., 1997. The Mid-Pleistocene climate transition: onset of 100 ka cycle lags ice volume build-up by 280 ka. *Earth Planet. Sci. Lett.* 151, 117–123.
- Munsterman, D., ten Veen, J., Menkovic, A., Deckers, J., Witmans, N., Verhaegen, J., Kerstholt-Boegehold, S., van de Ven, T., Busschers, F., 2019. An updated and revised stratigraphic framework for the Miocene and earliest Pliocene strata of the Roer Valley Graben and adjacent blocks. *Neth. J. Geosci.* 98, e8. doi:10.1017/njg.2019.10.
- Nishiizumi, K., 2004. Preparation of ^{26}Al AMS standards. *Nuclear Instruments and Methods in Physics Research B: Beam Interactions with Materials and Atoms* 223–224, 388–392.
- Nishiizumi, K., Winterer, E.L., Kohl, C.P., Lal, D., Arnold, J.R., Klein, J., Middleton, R., 1989. Cosmic ray production rates of ^{10}Be and ^{26}Al in quartz from glacially polished rocks. *J. Geophys. Res.* 94, 17907–17915.
- Nishiizumi, K., Imamura, M., Caffee, M., Southon, J., Finkel, R., McAninch, J., 2007. Absolute calibration of ^{10}Be AMS standards. *Nuclear Instruments and Methods in Physics Research B: Beam Interactions with Materials and Atoms* 258, 403–413.
- Peeters, A., Ek, C., 2018. Karstic Systems in Eastern Belgium: Remouchamps and Nôû Bleû. In: Demoulin, A. (Ed.), *Landscapes and Landforms of Belgium and Luxembourg*. Springer, pp. 115–138.

- Pissart, A., Harmand, D., Krook, L., 1997. L'évolution de la Meuse de Toul à Maastricht depuis le Miocène: corrélations chronologiques et traces des captures de la Meuse lorraine d'après les minéraux denses. *Géog. Phys. Quatern.* 51 (10), 267–284. doi:10.7202/033127ar.
- Pouclot, A., Juvigné, E., Pirson, S., 2008. The Rocourt Tephra, a widespread 90–74 ka stratigraphic marker in Belgium. *Quat. Res.* 70, 105–120. doi:10.1016/j.yqres.2008.03.010.
- Prodehl, C., Müller, S., Haak, V., 1995. The European Cenozoic rift system. In: Olsen, K.H. (Ed.), *Continental Rifts: Evolution, Structure, Tectonics*. In: *Developments in Geotectonics*. Elsevier, pp. 133–212.
- Quinif, Y., 1989. La notion d'étages de grottes dans le karst belge. *Karstologia* 13, 41–49.
- Quinif, Y., 2002. La grotte de Montfat: un jalon dans l'évolution de la vallée de la Meuse. *Karstologia* 40, 13–18.
- Quinif, Y., Hallet, V., 2018. The karstic system of Han-sur-Lesse. In: Demoulin, A. (Ed.), *Landscapes and Landforms of Belgium and Luxembourg*. Springer, pp. 139–158.
- Repka, J.L., Anderson, R.S., Finkel, R.C., 1997. Cosmogenic dating of fluvial terraces, Fremont River, Utah. *Earth Planet. Sci. Lett.* 152, 59–73.
- Ritter, J.R., Jordan, M., Christensen, U.R., Achauer, U., 2001. A mantle plume below the Eifel volcanic fields, Germany. *Earth Planet. Sci. Lett.* 186, 7–14.
- Rixhon, G., 2016. Reconstructing fluvial landscape evolution using terrestrial cosmogenic nuclide dating: achievements, limitations and applications. *Z. Dtsch. Ges. Geowiss.* 168, 169–182.
- Rixhon, G., Demoulin, A., 2010. Fluvial terraces of the Amblève: a marker of the Quaternary river incision in the NE Ardennes massif (Western Europe). *Z. Geomorphol.* 54 (2), 161–180. doi:10.1127/0372-8854/2010/0054-0008.
- Rixhon, G., Demoulin, A., 2018. The Picturesque Ardennian Valleys: Plio-Quaternary incision of the drainage system in the uplifting Ardennes. In: Demoulin, A. (Ed.), *Landscapes and Landforms of Belgium and Luxembourg*. Springer, pp. 159–176.
- Rixhon, G., Braucher, R., Bourlès, D., Siame, L., Bovy, B., Demoulin, A., 2011. Quaternary river incision in NE Ardennes (Belgium)-insights from $^{10}\text{Be}/^{26}\text{Al}$ dating of river terraces. *Quat. Geochronol.* 6, 273–284. doi:10.1016/j.quageo.2010.11.001.
- Rixhon, G., Bourlès, D.L., Braucher, R., Siame, L., Cordy, J.M., Demoulin, A., 2014. ^{10}Be dating of the main terrace level in the Amblève valley (Ardennes, Belgium): new age constraint on the archaeological and palaeontological filling of the Belle-Roche palaeokarst. *Boreas* 43, 528–542. doi:10.1111/bor.12066.
- Rixhon, G., Briant, R.M., Cordier, S., Duval, M., Jones, A., Scholz, D., 2017. Revealing the pace of river landscape evolution during the Quaternary: recent developments in numerical dating methods. *Quat. Sci. Rev.* 166, 91–113. doi:10.1016/j.quascirev.2016.08.016.
- Ruszkiczay-Rüdiger, Z., Braucher, R., Novothny, Á., Csillag, G., Fodor, L., Molnár, G., Madarász, B., ASTER Team, 2016. Tectonic and climatic control on terrace formation: coupling in situ produced ^{10}Be depth profiles and luminescence approach, Danube River, Hungary, Central Europe. *Quat. Sci. Rev.* 131, 127–147. doi:10.1016/j.quaint.2015.10.085.
- Sartégou, A., Bourlès, D.L., Blard, P., Braucher, R., Tibari, B., Zimmermann, L., Leanni, L., Aster Team Aumaitre, G., Keddadouche, K., 2018. Deciphering landscape evolution with karstic networks: a Pyrenean case study. *Quat. Geochronol.* 43, 12–29. doi:10.1016/j.quageo.2017.09.005.
- Schaller, M., von Blanckenburg, F., Veldkamp, A., Tebbens, L., Hovius, N., Kubik, P., 2002. A 30 000 yr record of erosion rates from cosmogenic ^{10}Be in middle European river terraces. *Earth Planet. Sci. Lett.* 204, 307–320.
- Schaller, M., von Blanckenburg, F., Hovius, N., Veldkamp, A., Van den Berg, M., Kubik, P., 2004. Paleocorrosion rates from cosmogenic ^{10}Be in a 1.3 Ma terrace sequence: response of the River Meuse to changes in climate and rock uplift. *J. Geol.* 112, 127–144.
- Stone, J., 2000. Air pressure and cosmogenic isotope production. *J. Geophys. Res.* 105, 23753–23759.
- Van Balen, R.T., Houtgast, R.F., Van der Wateren, F.M., Vandenberghe, J., 2000. Sediment budget and tectonic evolution of the Meuse catchment in the Ardennes and the Roer Valley Rift System. *Glob. Planet. Chang.* 27, 113–129. doi:10.1016/S0921-8181(01)00062-5.
- Westerhoff, W., Kemna, H., Boenigk, W., 2008. The confluence area of Rhine, Meuse, and Belgian rivers: Late Pliocene and Early Pleistocene fluvial history of the northern Lower Rhine Embayment. *Neth. J. Geosci.* 87 (1), 107–125.